

Isothermal Compressibility Maxima of Hydrogen Fluoride in the Supercritical and Superheated Vapor Regions

Barath Baburao and Donald P. Visco, Jr.*

Department of Chemical Engineering, Tennessee Technological University, Box 5013,
Cookeville, Tennessee 38505

Received: August 24, 2006; In Final Form: October 6, 2006

The highly nonideal behavior of hydrogen fluoride (HF) vapor has been considered to be the origin of its numerous vapor phase anomalies. In this work, we report one such potential vapor phase anomaly for HF. For a nonassociating substance like propane, the response functions go through a maximum only once in the supercritical region. However, for HF, when an association model is used to predict the isothermal compressibility (K_T), it exhibits a maximum in the supercritical region more than once, and this peak extends well in to the superheated vapor region upon decompression. This theoretical prediction is also supported by two other models recently developed for HF. Note that experimental values of K_T for HF have not been reported in the literature so far. Preliminary investigations on this K_T maximum for HF have suggested no reentrant spinodal, singularity-free scenario, or any additional first-order phase transition, unlike water, and, also, no λ (or higher-order phase) transitions, unlike liquid helium. However, this K_T peak is similar to the experimentally supported heat capacity (C_p) peak of HF which extends into the supercritical and superheated vapor regions. Similar to the C_p peak, which is understood based on vapor-phase clustering in HF, we relate K_T to the derivatives of enthalpy and entropy of the system. Also, we analyze some of the P – v – T experimental data that are available to provide an overview of the K_T behavior in the region of interest, and compare them with the model results. Finally, to explore the effect of including a distribution pattern for the oligomers, we report the results on a model that only includes association. Using this approach, we report K_T results with and without a Poisson-type oligomer distribution and show that the K_T appears once this distribution scheme is specified.

Introduction

Hydrogen fluoride (HF) has been a substance of considerable interest because of its unique properties and several useful applications.¹ It has been one of the most of extensively studied substances due to its relatively small size and the strength of its hydrogen bond in all phases.² This associating behavior makes its unusual physical and chemical properties similar to water instead of other hydrogen halides.³ However, unlike water, which associates in the liquid phase and shows limited association in the vapor phase (the compressibility factor of water vapor at 1 atm is 0.98),⁴ HF associates in both liquid and vapor phases (the compressibility factor of HF vapor at 1 atm is 0.29).⁵ This unusual vapor phase association has been considered to be the origin of its several anomalies such as high thermal conductivity of up to 0.6 W m^{−1} K^{−1},⁶ low enthalpy of vaporization (7.5 kJ mol^{−1} at normal boiling point), high vapor density, heat capacity maxima,^{6,7} etc. Much work has been dedicated to explain this vapor phase nonideality,^{1,6,8–11} and several models describing the vapor–liquid equilibrium for HF have been developed by incorporating association in both phases.^{2,5,12–18} However, the scarcity of experimental data on HF, due to its caustic and toxic nature, hampers the validation of these association models. This corrosive nature of HF has led to an increase in the number of theoretical studies, and henceforth, to an extent, some theoretical predictions have preceded the appearance of experimental data for HF.¹⁹ This trend is likely to continue in the future as well.

Thermodynamic models are computationally inexpensive and could act as a valuable tool in predicting properties that are not available in the literature and/or under conditions where performing experiments would be dangerous. Hence, it is essential to develop models with high predictive ability. These models can then be used to study properties or even potential anomalies that could aid in the molecular level understanding of the system of interest. In this work, we use an association model, whose predictive ability has been demonstrated earlier,^{20,21} to present and understand a heretofore unreported anomaly of HF. In particular, a maximum in the isothermal compressibility (K_T) for HF has been predicted by this model to be present in the superheated vapor (SHV) region and this extends into the supercritical (SC) region as well. To our knowledge, there is no modeling or experimental work reporting a K_T peak in the SHV region for *any* substance. However, a subcritical K_T peak has been reported in the liquid phase for helium,²² water,^{23,24} etc.

The paper is ordered as follows. First, we will introduce the K_T behavior for a nonassociating substance, propane, using the van der Waals equation of state (VDWEOS) to create a contrast for this HF work. We will then explain the K_T maximum that is exhibited by HF from the association model. After this, we will discuss some of the previous suggestions for the existence of these maxima and also examine the individual contributions for K_T from this model. We also provide the conditions that are to be satisfied for the existence of this K_T peak for any thermodynamic model. We then analyze the results based on

* To whom correspondence should be addressed. E-mail: dvisco@tntech.edu. Phone: 931 372 3606. Fax: 931-372-6352.

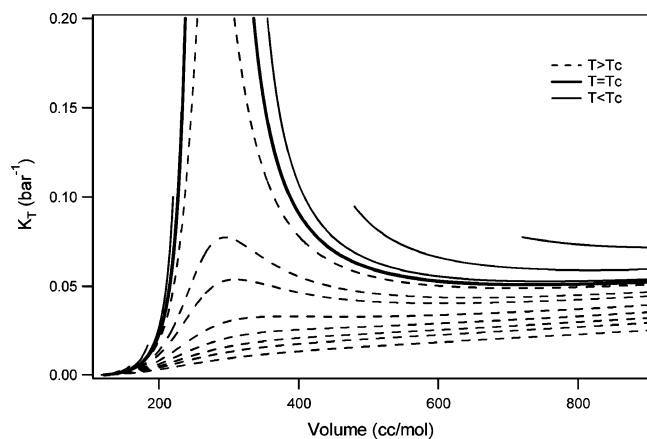


Figure 1. K_T results for propane using the VDWEOS.

thermodynamic relationships and vapor phase association in HF, and relate the K_T maximum in terms of changes in enthalpy and entropy of the system. We also analyze the available P – v – T data in the literature to comment on the existence of the K_T peak for HF. Finally, we demonstrate the effect of including an association scheme into an ideal model on the generation of a peak in K_T .

K_T Results for Propane from the VDWEOS

The isothermal compressibility is defined as follows²⁵

$$K_T = -\frac{1}{v} \left(\frac{\partial v}{\partial P} \right)_T \quad (1)$$

where v is the specific volume, P is the absolute pressure, and the subscript T is the absolute temperature at which K_T is calculated.

As is well-known, the slope, $(\partial P/\partial v)_{T=T_c}$, and second derivative, $(\partial^2 P/\partial v^2)_{T=T_c}$, of the P – v isotherms are zero at the critical point. Thus, on the basis of the definition of K_T , similar to other response functions, it diverges as the critical point is approached. Just above the critical point, the P – v isotherm goes through a concavity change. Hence, K_T goes through a maximum (or a peak) at temperatures moderately above the critical temperature. Eventually, the peak is suppressed at temperatures well above the critical point as the ideal gas limit is approached.

To understand this behavior, for nonassociating fluids, the K_T values were evaluated for propane using the VDWEOS. Figure 1 shows the evolution of the K_T peak as a function of volume in both the subcritical and SC regions. The K_T values in the subcritical regions are shown by solid lines, whereas the SC regions are indicated by dashed lines. The bold solid line indicates the K_T results at the critical point. As one can see, the K_T isotherms peak in the SC region and will, eventually, go off to infinity at the ideal gas limit.

HF Association Model

As suggested earlier, HF is a substance which shows strong association in all phases; hence, cubic equations of state are ill-equipped to describe this substance. Of the several models^{2,5,12–18} that describe the vapor-phase properties of HF at a reasonably accurate level, the modified association + equation of state (AEOS-VK) model was chosen to perform these K_T calculation.¹⁵ This is due to its relative computational simplicity, as well as its ability to capture some of the unique features of HF such as the peak in the heat of vaporization,

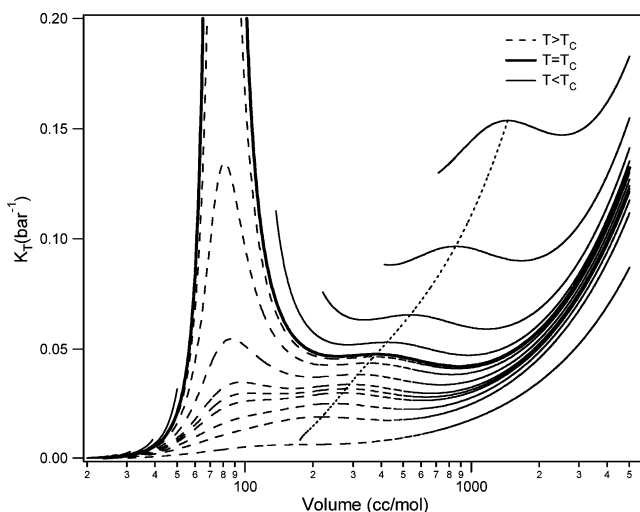


Figure 2. K_T results for HF using the AEOS-VK model. The model predicts the critical temperature to be 473.1 K. Note that the dotted line, which shows the locus of second maxima, ends at 668 K.

heat capacity maximum, etc. Before discussing the K_T results for HF, we will briefly review the AEOS-VK model.

The AEOS-VK model has its origin from Anderko's¹³ association + equation of state (AEOS), which is best described in terms of the compressibility factor (Z). Similar to the decomposition of second virial coefficients,²⁶ the compressibility factor is divided into two parts, a chemical part (Z^{ch}) and a physical part (Z^{ph}), and accordingly, it can be written as

$$Z = Z^{\text{ph}} + Z^{\text{ch}} - 1 \quad (2)$$

The Z^{ch} term describes the association interactions including the formation of clusters through appropriate association schemes, while Z^{ph} describes all possible nonspecific interactions between these clusters, including the monomers, using a cubic equation of state (here, Peng–Robinson was used, PREOS). The Z^{ch} term was calculated assuming consecutive self-association reactions, with the equilibrium constant for each reaction obtained as a product of a distribution function and the dimerization constant. We refer the reader to the original work^{15,27} for the analytical formulations and parameter values for this equation of state.

K_T for HF from the AEOS-VK Model

Figure 2 shows the K_T behavior for HF from the AEOS-VK model. The legends are similar to Figure 1. As one can see, unlike propane, K_T in the SHV region for HF shows a maximum, and this extends into the SC region as well. Above the critical point, the thermodynamic response functions (e.g., constant pressure heat capacity (C_p), K_T , volume expansivity (α_p), etc.) that are derivatives of state functions exhibit a maximum. These response functions diverge as the critical point is approached. If one plots the lines of maxima of the different response functions in the SC region, in the P – T plane, it can be seen that they approach the critical point asymptotically. This asymptotic line is sometimes called as the Widom line²⁸ (here, the AEOS-VK model predicts that the line ends at 474.6 K). For a nonassociating substance, like propane, the response functions goes through a maximum only once in the SC region (as in Figure 1), and these lines of maxima approach asymptotically through the Widom line as expected. However, for HF as shown in Figure 2, K_T results from the AEOS-VK model shows two maxima in the SC region. When the system is

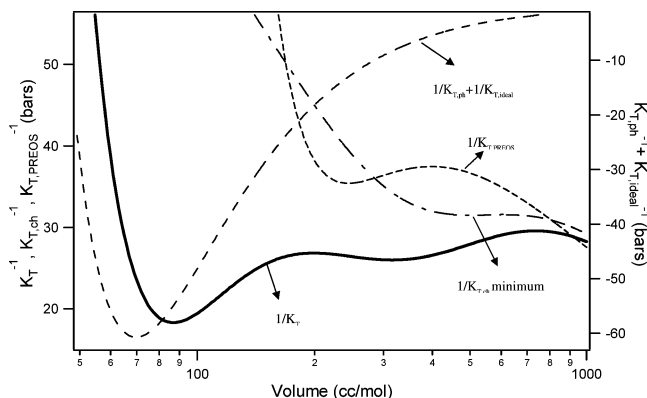


Figure 3. Individual contributions for $1/K_T$ for HF from the AEOS-VK model at 490 K.

decompressed, this additional peak extends well into the SHV region. The dotted line traces the locus of the K_T maximum in the SHV and SC region. While the response functions exhibit a maxima and approach the critical point through the Widom line, the second maxima does not occur at the same point. As such, α_P does not exhibit this second maxima. On the other hand, both the C_P and K_T from the AEOS-VK model show this additional peak that extends from the SHV region and well in to the SC region.

Prior Studies on the K_T Peak

As suggested earlier, K_T maxima have been previously reported for water and He. Thus, in order to examine the existence of a similar scenario, we examined the explanations that were established for water K_T maxima in the subcritical region.^{23,24,29–32} These studies explain the K_T maxima in three different ways: (i) retracing spinodal scenario, (ii) singularity-free interpretation, and (iii) first-order phase transition between two distinct liquid phases. For HF, using the AEOS-VK model, none of these scenarios were observed. Also, attempts at exploring this second K_T maximum based on λ or higher-order phase transitions, like in liquid He,²² were not fruitful.

K_T Individual Contributions

Since we were unable to make use of what has been reported earlier on the liquid-phase K_T maxima, the additional peak was examined by evaluating the individual contributions for K_T from the AEOS-VK model. Like the compressibility factor, K_T for HF from the AEOS-VK model can also be described in terms of physical and chemical parts as shown below

$$\frac{1}{K_T} = \frac{1}{K_{T,ph}} + \frac{1}{K_{T,ph}} + \frac{1}{K_{T,ideal}} \quad (3)$$

The individual contributions are obtained by substituting the corresponding compressibility factors in the equation below,

$$\frac{1}{K_T} = \frac{RT}{v} \left[Z - v \left(\frac{\partial Z}{\partial v} \right)_T \right] \quad (4)$$

Figure 3 shows the individual K_T^{-1} contributions for an SC isotherm at 490 K where two peaks are reported. Reciprocal functions exhibit a minimum when the original function goes through a maximum. As one can see, there are two minima in K_T^{-1} (solid line) that corresponds to the two peaks that were shown in Figure 2. Investigating the individual contributions helps us to understand the effect of association through the chemical part. The sum of the physical and ideal parts of K_T^{-1}

(i.e., $K_{T,ph}^{-1} + K_{T,ideal}^{-1}$), which is indicated by the dashed line, shows only one minimum. This minimum corresponds to the first minimum in the SC region (the one from the singularity). On the other hand, $K_{T,ch}^{-1}$ (dotted and dashed line) shows a minimum that corresponds to the second K_T^{-1} minimum in the SC region. This second minimum is seen in the SHV region under subcritical conditions. Therefore, even if the association is not specified by the chemical part, the equation of state would exhibit the first peak in K_T as in propane, while this is not so with the second peak. To illustrate this, the K_T results for HF from just a conventional equation of state with no association (the PREOS) are also reported in Figure 3. As expected, similar to propane, the PREOS for HF shows only one peak in the SC region. The existence of a minimum in $K_{T,ch}^{-1}$, and the fact that the second peak is neither present for a nonassociating substance such as propane nor for HF from PREOS, indicates that the SHV peak in the subcritical region and the second peak in the SC region is a phenomenon that is exhibited only due to the chemical part, hence the association.

Conditions for K_T Peak

Now that we understand the existence of a K_T peak in the SHV region, it would be apt to derive the conditions that are satisfied at this point and relate it to any equation of state. The slope of K_T with respect to pressure or volume is zero, i.e.,

$$\left(\frac{\partial K_T}{\partial v} \right)_T = \left(\frac{\partial K_T}{\partial P} \right)_T = 0 \quad (5)$$

at the point where the peak exists. On the basis of the definition of K_T in eq 1, we can derive the condition that should be satisfied for the K_T peak to occur. From either of the forms above, we can arrive at the condition,

$$\left(\frac{\partial P}{\partial v} \right)_T + v \left(\frac{\partial^2 P}{\partial v^2} \right)_T = 0 \quad (6)$$

Excluding an analysis based on the singularity at the critical point (where both terms in eq 6 are zero), for a thermodynamically stable peak to occur not at the critical point, the $(\partial P/\partial v)_T$ and $v(\partial^2 P/\partial v^2)_T$ terms must be equal and opposite. For nonassociating fluids such as propane, this condition is satisfied (at constant temperature) for a peak only once in the SC region and never in the subcritical region. But for HF, from the AEOS-VK model, this scenario for a peak is satisfied twice in the SC region and once in the subcritical region (at constant temperature).

Using eq 6, we can trace the locus of points where K_T exhibits a maximum. Figure 4 ($P-v$ plane) and Figure 5 ($P-T$ plane) show the locus of the K_T maximum from the AEOS-VK model in both the subcritical and SC regions. In Figures 4 and 5, $L-C-V$ is the phase coexistence curve, with C being the critical point, L representing the liquid region, and V representing the vapor region at near ideal conditions. The locus of the first K_T peak in the SC region is indicated as $C-A$, and the second peak, which extends in to the SHV region, is indicated as $V-A^*$. The Widom line is indicated by the $C-W$ that is circled in the embedded plot in Figure 5. The locus of the C_P maximum in the SC region is indicated as $C-B$, whereas the second peak that extends into the SHV region is indicated by $V-B^*$. The locus of the α_P peak is indicated by $C-D$. As one can see, the Widom line occurs only once, which implies no second critical point (as in water).²⁸

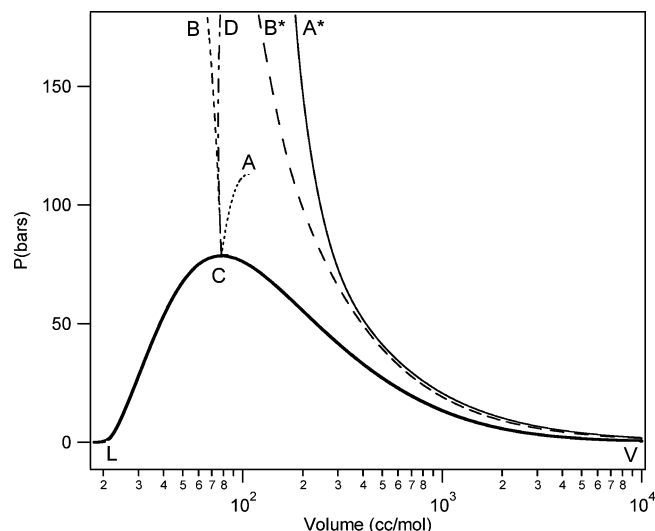


Figure 4. Loci of the K_T , C_P , and α_P peak in the P - v plane for HF from the AEOS-VK model.

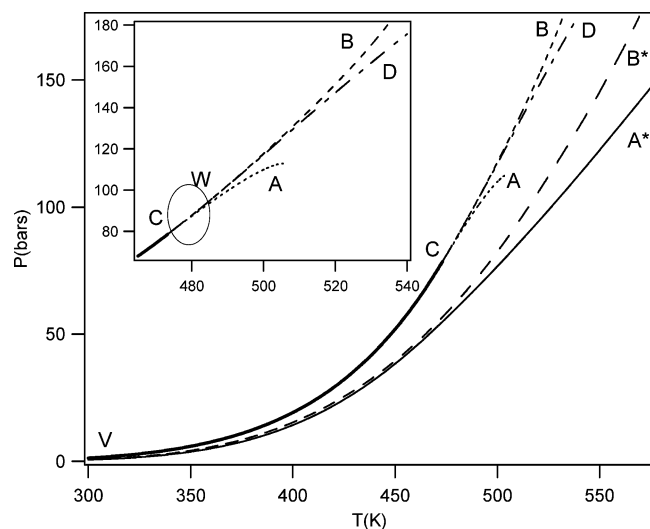


Figure 5. Loci of the K_T , C_P , and α_P peak in the P - T plane for HF from the AEOS-VK model.

C_P and K_T Comparison

As suggested earlier, reporting a maximum in a response function for HF in the SHV region is not new. The C_P for HF has been reported to go through a maximum in the SHV region.³³ The peak in C_P can be understood in terms of enthalpy changes that are associated with the bond breaking that occurs in the SHV region for HF. We know that HF is a substance that shows association in all phases with the existence of higher order polymers in the form of chains as well as ring aggregates. Approximately 6–8 kcal/mol of energy is released for every broken hydrogen bond in HF.³⁴ The enthalpy and, hence, its derivative ($C_P = (\partial H/\partial T)_P$) is highly dependent on this degree of association. Rapid changes in the association patterns in the SHV region at constant pressure cause the system to go from a high associated state to a low associated state, and this behavior mimics the enthalpy changes that would occur during a phase transition. Hence, due to this pseudo phase change from a highly associated state to a near ideal phase, the enthalpy change is large and, thus, the C_P goes through a maximum. This is the case with the entropy of the system as well; the rapid change in the degree of association also increases the entropy as the system undergoes this pseudo phase transition ($C_P = T(\partial S/\partial T)_P$). Hence, under constant pressure conditions, the enthalpy, entropy,

and the mean association number ($\chi = 1/Z^{\text{ch}}$) show a marked change along the region where the C_P peak is reported.

While the relationship between the C_P maximum and the vapor phase association, to a certain extent, is direct, this is not the case with K_T . We know that $G = A + Pv$, where G and A are the Gibbs and Helmholtz free energies, respectively. Differentiating this partially with respect to molar volume at constant temperature and using $P = -(\partial A/\partial v)_T$ leads us to

$$\left(\frac{\partial G}{\partial v}\right)_T = -\frac{1}{K_T} \quad (7)$$

Qualitatively, G' mimics the behavior of K_T showing peaks under conditions where the K_T peak is reported. Now, we can rewrite G in terms of enthalpy and entropy as, $G = H - TS$, which, in turn, helps us to connect K_T to its derivatives.

$$\left(\frac{\partial G}{\partial v}\right)_T = \left(\frac{\partial H}{\partial v}\right)_T - T\left(\frac{\partial S}{\partial v}\right)_T \quad (8)$$

Unlike C_P , K_T is related to the combination of the derivatives of both the enthalpy and entropy. Further, both H and S are stronger functions of temperature than volume. At constant temperature, in the region where the K_T or C_P maximum is seen, the changes in H and S are not as prominent as they are in the region where the C_P peak is seen at constant pressure. Therefore, in order to understand the K_T maximum and to study the changes in enthalpy and entropy that are associated with the vapor phase association changes at constant temperature, it is necessary to examine the behavior of the first and second derivatives of enthalpy and entropy with respect to volume.

Even though the derivative functions of H and S with respect to volume at constant temperature behave in a similar fashion qualitatively, it is H' and $-TS'$ that are used to calculate K_T , and these functions behave quite oppositely. While H' increases, $-TS'$ decreases due to the breaking of hydrogen bonds in the SHV region. Since K_T is the algebraic sum of these two terms, it could either have a minimum or a maximum or could be a monotonically increasing function based on the concavity changes of the derivative functions. These changes in the derivative functions can cancel each other out, resulting in a flat region in K_T instead of a peak or can occur in the two-phase region which would prevent them from being observed in the SHV region.

Figure 6 shows the behavior of the second derivative functions of enthalpy and entropy from both the AEOS-VK model and the PREOS alone (no association) for HF at 490 K. It is clear that the second derivatives of the enthalpy and entropy terms from the AEOS-VK model show a concavity change in the region where the second peak in G' (hence K_T) is reported. On the other hand, this is not the case for the PREOS results, where no concavity changes are observed in the SC region for those two second-derivative terms.

K_T Results from Available Experimental Data

To explore the existence of this second K_T peak from the experimental studies, we analyzed the available density data in the literature. A useful approach to analyze this data is to plot the natural logarithm of the volume versus the pressure at constant temperature (since $K_T = -(\partial \ln v/\partial P)_T$). If an inflection point in the data is realized, this is indicative of a peak in K_T . With that in mind, we explored the SC P - v data of Franck et al.³⁵ but noticed no inflection point at all. It is to be noted, however, that the volumes encompassed by this data set do not intercept either AEOS-VK predicted K_T peak. On

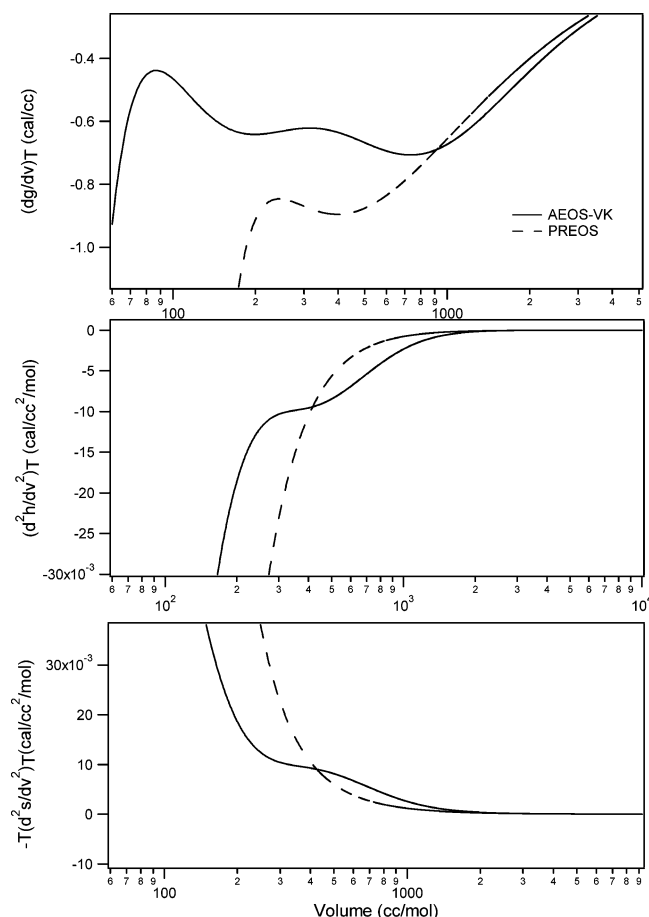


Figure 6. Behavior of the derivative functions from the AEOS-VK model and the PREOS for HF at 490 K.

the other hand, the SC P – v isotherms listed by another work³⁴ do encompass the volume region where only the first peak is likely to occur. These experimental data do exhibit a clear inflection point when one plots $\ln v$ as a function P .

In the SHV region, of the several experimental P – v isotherms available,^{8,9,36,37} three isotherms (299.15, 205.15, and 311.15 K) overlap the volume region where the K_T peak is reported by the AEOS-VK model. When one plots this isothermal data as the natural logarithm of the volume versus the pressure, it is not clear via inspection if an inflection point exists. Also, owing to the fluctuations in the experimental data as presented, numerical differentiation to glean a peak in K_T would not be effective. Thus, one can potentially fit the data with a functional form and then take the derivative to determine if a peak in K_T exists. However, owing to the small magnitude of the peak predicted at this state, such a procedure is ambiguous. To illustrate this, we use two polynomial expressions to fit the experimental data³⁷ at 305.15 K. The parameters of these two expressions and their absolute average deviation (AAD, %AAD = $(100/N_{\text{data}}) \sum_{i=1}^{N_{\text{data}}} \{[(\ln(v_{\text{exp}}) - \ln(v_{\text{poly}}))/\ln(v_{\text{exp}})]\}$) values are listed in Table 1. Figure 7 shows the results from these two polynomial expressions as well as the AEOS-VK model. As one can see, the polynomial fits basically overlap each other,

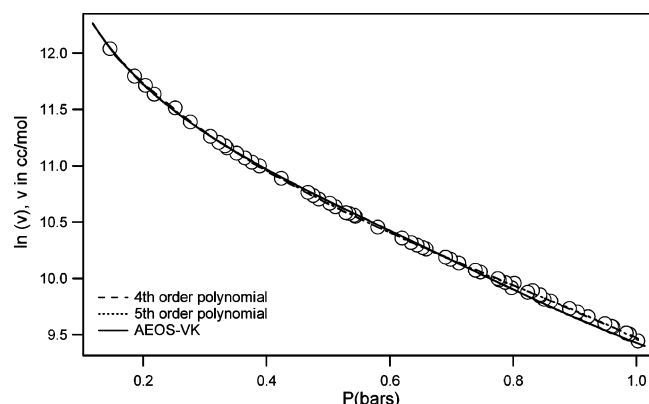


Figure 7. P – v – T results from the polynomial fit and the AEOS-VK model at 305.15 K. Empty symbols indicate the experimental data.³⁷

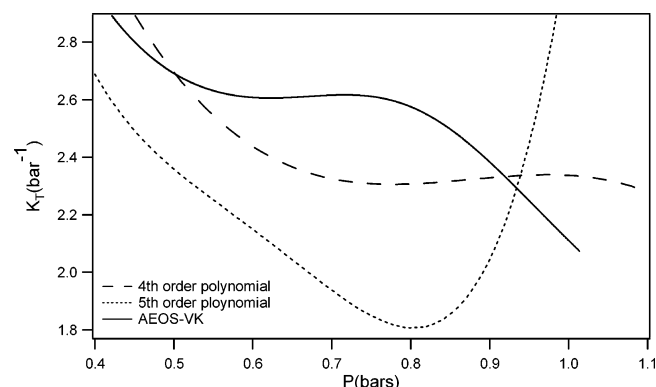


Figure 8. K_T results from the polynomial fit and AEOS-VK model.

though inspection of the regression coefficients in Table 1 provides a different story. These differences are clearly seen in Figure 8 wherein the fourth-degree polynomial shows a peak while the fifth-degree one does not. Thus, one cannot draw a conclusion either way about the existence of a K_T peak from this data. Additional and more precise measurements in the SHV region as well as molecular simulations under these experimental conditions would bring more information that would aid in understanding the existence of this K_T peak for HF.

Other Association Models

The maximum in K_T in the SHV is not just a feature that is exhibited by the AEOS-VK model alone. Two other models, the AEOS¹³ model and the Lee–Kim model,¹⁸ which describes association in HF through chemical and physical parts, as in AEOS-VK, show this K_T maximum in the SHV region. While the AEOS model shows these maxima in the SHV and SC regions, the Lee–Kim model exhibits this phenomenon only in the SHV region from 350–395 K and shows only one maximum in the SC region. Fundamentally, from an association perspective, the AEOS and AEOS-VK models use an unconstrained yet biased association scheme, while the Lee–Kim model uses an association scheme that allows the formation of monomers, dimers, hexamers, and octamers only. Even though the Lee–Kim model shows high accuracy in correlating the

TABLE 1: Parameters and AAD Values for the Polynomial Fit at 305.15 K^{37a}

polynomial fit	parameters						% AAD
	A_1	A_2	A_3	A_4	A_5	A_6	
fourth-degree	0	2.21988	−7.77254	10.07766	−8.05317	13.001	0.0710
fifth-degree	−9.54058	29.8296	−37.7227	−25.0803	−11.462	13.2763	0.0491

^a Here, $\ln v = A_1 P^5 + A_2 P^4 + A_3 P^3 + A_4 P^2 + A_5 P + A_6$ (P in bars, v in cubic centimeters per mole).

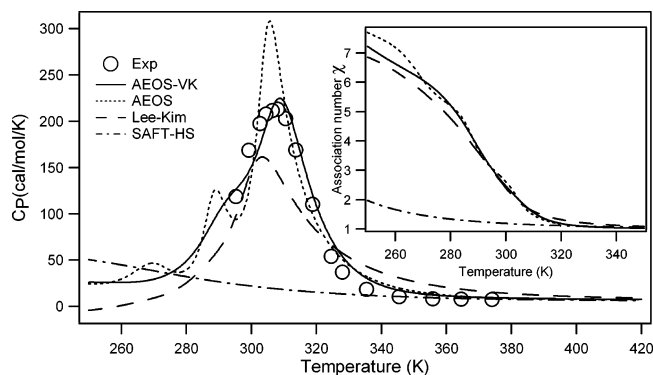


Figure 9. C_p results for pure HF from the AEOS-VK, AEOS, SAFT-HS, and Lee-Kim models at 721 mmHg.

phase equilibrium properties at saturation, away from saturation, it fails to predict the C_p results at the same level. On the other hand, the results from the SAFT-HS model do not show *any* maxima in K_T in the SHV region. Considering the fact that SAFT-HS was not able to reproduce features like the heat of vaporization maxima and C_p maximum,^{38–40} this is not surprising.

Figure 9 shows the C_p results from the AEOS-VK, AEOS, SAFT-HS, and Lee-Kim models at 721 mmHg.³³ As one can see, the AEOS-VK model predicts the C_p results with the highest level of accuracy when compared to the other models. Even though the AEOS model predicts the C_p peak with a reasonable level of accuracy, it shows unphysical shoulders that are not supported by the experimental data and overpredicts the peak value. On the other hand, the Lee-Kim model does not show these unphysical shoulders but underpredicts the peak. This is likely attributed to the association scheme that was adopted during the correlation stage of this model. One can speculate that the less accurate C_p prediction (smaller peak) from this model gives rise to the limited region where the K_T peak is realized (350–395 K). Even more so, the SAFT-HS approach does not show a peak in C_p and, likewise, shows no second K_T peak at all.

Significance of the Oligomer Distribution

The low C_p peak of the Lee-Kim model and the disappearance of the K_T SHV peak would seem to illustrate the importance of the *type* of oligomer distribution used in the modeling. The conjecture is that it is not good enough just to add association to a model or even to add the proper oligomers, but one must obtain a realistic distribution of these oligomers. The fact that a coarse-grained measure of association, as viewed through the association number, is misleading in the analysis of these response functions is easily seen in the inset of Figure 9. Here, we plot the association number for all of the models as a function of temperature. While all of the models that predict a peak in C_p exhibit the same general association number curve, they provide widely different results for both C_p and K_T .

To explore the above oligomer distribution issue further, we next focus directly on the association alone through the ideal association model (IAM). We refer the reader elsewhere for a detailed description of this approach.^{41–43} In brief, the IAM is a very simple molecular model that includes only association interactions by placing square-well sites in otherwise ideal particles.

Similar to the established approach to study association, the IAM model describes the formation and destruction of oligomers as a set of chemical reactions. Applying the chemical equilibrium conditions and from the ideal partition function, the number

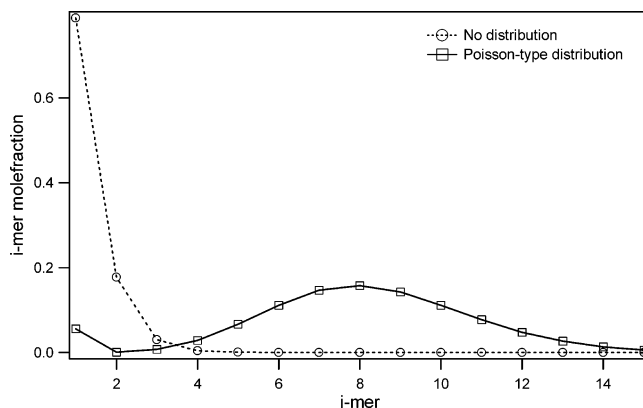


Figure 10. Distribution of oligomers from the IAM model with and without a Poisson-type oligomer distribution.

of molecules of species i is represented by

$$N_i = N_1^i q_i \quad (9)$$

where q_i is the internal configurational integral of an *i*-mer that plays the role of a reaction constant.⁴² For a system which does not have any prespecified distribution of oligomers (i.e., $q_i = q^{i-1}$; $q = q_2$), N_i can be rewritten as

$$N_i = \frac{N}{A} \left(1 - \frac{1}{2A} (H - 1) \right)^i \quad (10)$$

where N is the total number of monomers assuming no association, $H = (4A + 1)^{1/2}$ and $A = qN/V = \rho V_{\text{eff}} \exp(\beta\epsilon)$ with $\beta = 1/K_B T$ where ϵ is the energy of interaction. $V_{\text{eff}} = 4/3\pi R^3$ is the bonding volume for two molecules of radius R , and $\rho = N/V$ is the number density.⁴¹ As we can see, the oligomer distribution depends upon temperature and density through A , through which association is defined. Finally, the equation of state of these noninteracting oligomers is given by $\beta P = \rho[(\sum_i N_i)/N]$.

In order to explore the effect of a specific oligomer distribution, we modified the IAM to impose a Poisson-type distribution which is incorporated in q_i in a fashion similar to what was proposed by the AEOS model. Thus, q_i is given by

$$q_i = f(i) q^{i-1}, \quad f(j) = \frac{\kappa^{j-1}}{(j-1)!} \quad (11)$$

In addition to the two parameters ($R = 0.5052 \times 10^{-8}$ Å, $\epsilon = 2.8492 \times 10^{-20}$ J molecule⁻¹) in the original IAM model, a third parameter ($\kappa = 710$) was introduced to incorporate a Poisson-type oligomer distribution. Note that these parameters were chosen not to map onto any real system but just to provide a distribution for illustrative purposes.

Using this IAM model, we report the K_T results with and without the Poisson-type distribution. Except for the inclusion of the third parameter, κ , the other two parameters are set to be the same in both cases. The N_i distribution from both cases is shown in Figure 10 at 1 bar and 275 K. The lines between the markers serve as a guide for the eye. When one does not use the imposed distribution, the monomer is the dominating oligomer and the importance of other oligomers falls monotonically. When one imposes the Poisson-type distribution, the dominant oligomer becomes the 8-mer. The K_T results from both scenarios are shown in Figure 11. As one can see, with no prescribed distribution scheme, the IAM model does not show any K_T peak. However, when an imposed distribution is used, a K_T peak exists. Once again, this suggests that it is not just the

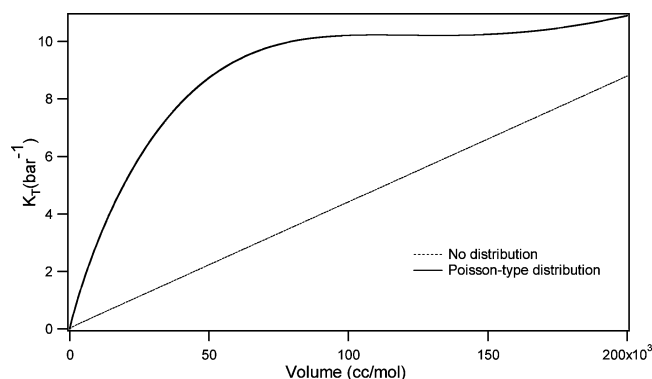


Figure 11. K_T results from the IAM model.

types of oligomers that are allowed to form but their specific distribution that gives rise to peaks in these response functions.

Summary

As previously mentioned, sometimes modeling or theoretical predictions for HF have preceded their experimental verification. In this work, we have explored the potential existence of a second peak in the isothermal compressibility of HF that extends from the SHV region into the SC region. The finding that the models which predict this phenomenon also capture the experimentally supported C_P maximum in the SHV region provides some optimism that such a K_T peak is not an artifact of the model.

The enthalpy and entropy changes that occur due to the rapid changes in the association patterns in the SHV region for HF are prominent under constant pressure conditions. These changes mimic the changes that would occur during a phase transition, thereby resulting in a C_P peak. When these structural changes are induced by an increase in volume under isothermal conditions, the changes in enthalpy and entropy are not as prominent as those under nonisothermal conditions. However, in both cases, the responses functions (C_P and K_T) acquire a maximum, indicating the changes in association patterns in the SHV and SC regions.

In this work, we also analyzed the experimental data that are available in the SC and SHV regions. In both regions, the available data were not sufficient to provide any conclusive evidence for the existence of this additional peak. We also examine the importance of oligomer distributions and their effect on the response functions through examining HF equations of state as well as a model that only includes association. In both scenarios, the specific distribution of the oligomers available gave rise to much different results.

At this point, the existence of this second peak in the isothermal compressibility of HF is only speculation. However, molecular-level simulations can provide a potential window into exploring this phenomenon even further. In a recent work from Jedlovsky and co-workers,¹⁹ molecular simulation results for HF using a new polarizable potential model (and earlier models) show the first K_T peak in the SC region where the AEOS-VK model peak is also reported. Additionally, and though not reported directly in that work, there is some evidence that a second peak might exist as well for some of the models. Such a result provides motivation for additional experiments and/or molecular simulation under the conditions where this second peak is suspected, both in the SC and SHV regions.

Acknowledgment. This work was supported by the American Chemical Society, Petroleum Research Fund (PRF42227-

AC9) and the Center for Manufacturing Research, Tennessee Technological University. We also would like acknowledge the Computer Aided Engineering Laboratory Personnel, Tennessee Technological University for providing the computational facilities for this work.

References and Notes

- (1) Simons, J. W.; Bouknight, J. J. *Am. Chem. Soc.* **1932**, *54*, 129.
- (2) Galindo, A.; Whitehead, P. J.; Jackson, G. J. *Phys. Chem. B* **1997**, *101*, 2082.
- (3) Simons, J. H. *Fluorine Chem.* **1950**, *1*, 225.
- (4) Van Ness, H. C. *Pure Appl. Chem.* **1995**, *67*, 859.
- (5) Kao, C. P. C.; Paulaitis, M. E.; Sweany, G. A.; Yokozeiki, M. *Fluid Phase Equilib.* **1995**, *108*, 27.
- (6) Franc, E. U.; Spalhoff, W. *Naturwissenschaften* **1953**, *40*, 580.
- (7) Quack, M.; Schmitt, U.; Suhm, M. A. *Chem. Phys. Lett.* **1993**, *208*, 446.
- (8) Jarry, R. L.; Davis, W. J. *Phys. Chem.* **1953**, *57*, 600.
- (9) Long, R. W.; Hilderband, J. H.; Morrell, W. E. *J. Am. Chem. Soc.* **1943**, *65*, 182.
- (10) Schotte, W. *Ind. Eng. Chem. Proc. Des. Dev.* **1980**, *19*, 432.
- (11) Beckerdite, J. M.; Powell, D. R.; Adams, E. T. *J. Chem. Eng. Data* **1983**, *28*, 287.
- (12) Twu, C. H.; Coon, J. E.; Cunningham, J. R. *Fluid Phase Equilib.* **1993**, *86*, 47.
- (13) Lencka, M.; Anderko, A. *AIChE J.* **1993**, *39*, 533.
- (14) Economou, I. E.; Peters, C. J. *Ind. Eng. Chem. Res.* **1995**, *34*, 1868.
- (15) Visco, D. P.; Kofke, D. A. *Ind. Eng. Chem. Res.* **1999**, *38*, 4125.
- (16) Gillespie, P. C.; Cunningham, J. R.; Wilson, G. M. *AIChE Symp. Ser.* **1985**, *81*, 41.
- (17) Wilson, L. C.; Wilding, W. V.; Wilson, G. M. *AIChE Symp. Ser.* **1989**, *85*, 51.
- (18) Lee, J.; Kim, H. *Fluid Phase Equilib.* **2001**, *190*, 47.
- (19) Partay, L.; Jedlovsky, P.; Vallauri, R. *J. Chem. Phys.* **2006**, *124*, 184504/1.
- (20) Visco, D. P. The Thermodynamic and Molecular Modeling of Hydrogen Fluoride. Ph.D. Dissertation, State University of New York at Buffalo, 1999.
- (21) Baburao, B.; Visco, D. P. *Ind. Eng. Chem. Res.* **2002**, *41*, 4863.
- (22) Grilly, E. R. *Phys. Rev.* **1966**, *149*, 97.
- (23) Sastry, S.; Debenedetti, P. G.; Francesco, S.; Stanley, H. E. *Phys. Rev. E* **1996**, *53*, 6144.
- (24) Sciortino, F.; Poole, H. P.; Essman, U.; Stanley, H. E. *Phys. Rev. E* **1997**, *55*, 727.
- (25) Smith, J. M.; Van Ness, H. C.; Abbott, M. M. *Introduction to Chemical Engineering Thermodynamics*, sixth ed.; McGraw-Hill: New York, 2001.
- (26) Lambert, J. D. *Discuss. Faraday Soc.* **1953**, *15*, 226.
- (27) Visco, D. P.; Kofke, D. A. *Ind. Eng. Chem. Res.* **2000**, *39*, 242. In addition to this, an additional term $\lambda_7 = -p_4 p_5 / p_5 + p_7 p_8 / p_8$ has to be included to the λ^{ch} term of the fugacity coefficient.
- (28) Xu, L.; Kumar, P.; Buldyrev, S. V.; Chen, S. H.; Poole, P. H.; Sciortino, F.; Stanley, H. E. *Proc. Natl. Acad. Sci. U.S.A.* **2005**, *102*, 16558.
- (29) Speedy, R. J.; Angell, C. A. *J. Chem. Phys.* **1976**, *65*, 851.
- (30) Speedy, R. J. *J. Phys. Chem.* **1982**, *86*, 982.
- (31) Truskett, M. T.; Debenedetti, P. G.; Sastry, S.; Torquato, S. *J. Chem. Phys.* **1999**, *111*, 2647.
- (32) Jedlovsky, P.; Vallauri, R. *Phys. Rev. E* **2003**, *67*, 011201.
- (33) Frank, E. U.; Meyer, F. Z. *Elektrochem.* **1959**, *63*, 571.
- (34) Franck, E. U.; Spalhoff, W. Z. *Electrochem.* **1957**, *61*, 348.
- (35) Franck, E. U.; Wiegand, G.; Gerhardt, R. *J. Supercrit. Fluid* **1999**, *15*, 127.
- (36) Strohmeier, W.; Briegleb, G. Z. *Electrochem.* **1953**, *57*, 662.
- (37) Fredenhagen, K. Z. *Anorg. Allg. Chem.* **1934**, *218*, 161.
- (38) Visco, D. P.; Kofke, D. A. *Fluid Phase Equilib.* **1999**, *37*, 158.
- (39) Juwono, E. Engineering Modeling of Hydrogen Fluoride and Water Mixture Using Statistical Associating Fluid Theory. Master's Thesis, State University of New York, Buffalo, New York, 1998.
- (40) Galindo, A.; Burton, S. J.; Jackson, G.; Visco, D. P.; Kofke, D. A. *Mol. Phys.* **2002**, *100*, 2241.
- (41) Visco, D. P.; Kofke, D. A. *J. Chem. Phys.* **1999**, *110*, 5493.
- (42) van Roij, R. *Simple Theories of Complex Fluids*. Ph.D. Dissertation, FOM-Institute for Atomic and Molecular Physics, Amsterdam, 1996.
- (43) van Roij, R. *Phys. Rev. Lett.* **1996**, *76*, 3348.